MINERAL RESOURCES TASMANIA

2023

Lily-Lagoon 3D Model

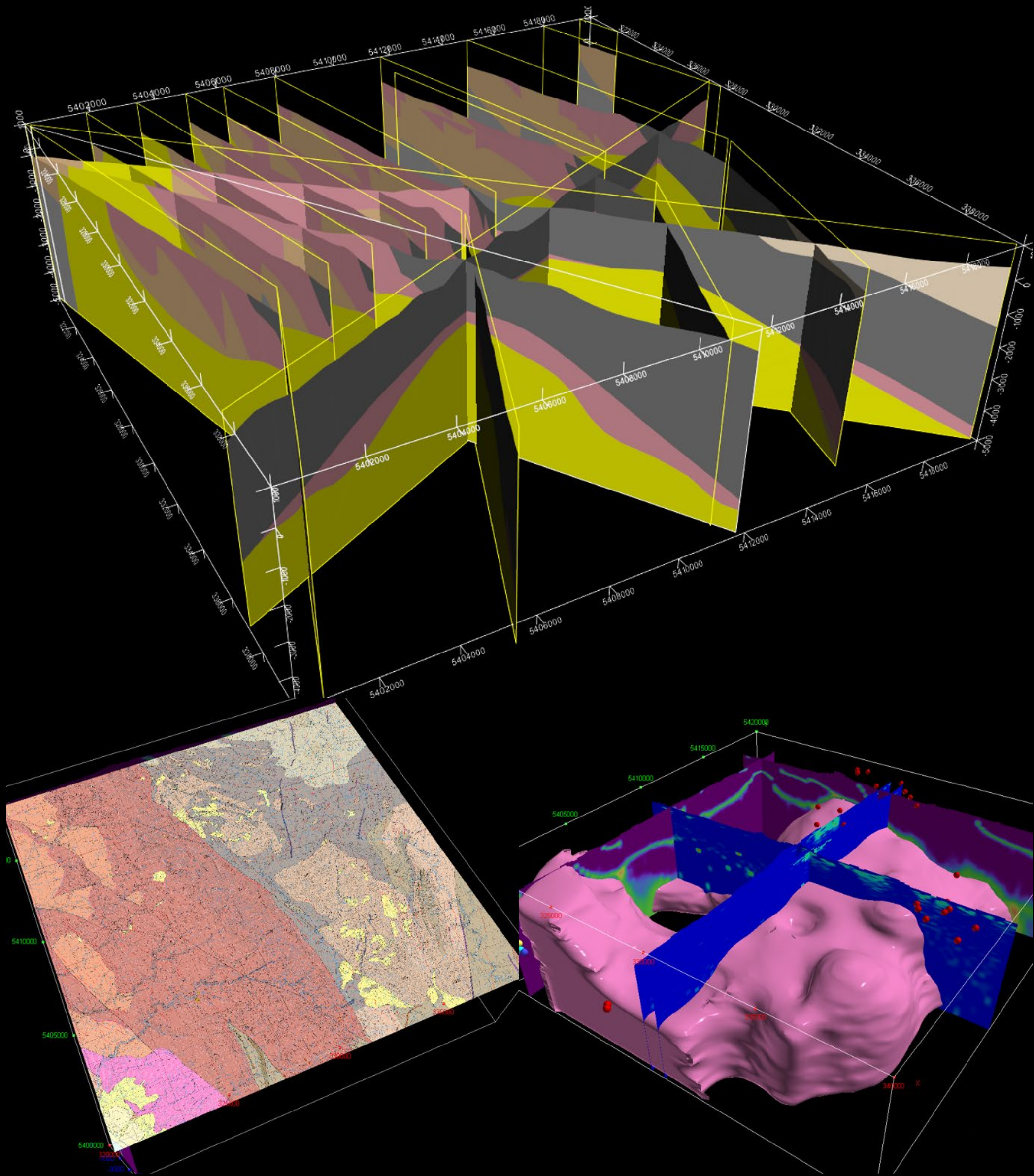

Author: D. Bombardieri, M. Duffett, J. L. Everard and G. V. Cumming

Date: 20/02/2023

Email: info@mrt.tas.gov.au

Website: www.mrt.tas.gov.au

REPORT No.: TR35

Geological Survey Explanatory Notes

Tasmanian Government

Mineral Resources Tasmania
Department of State Growth

Lily-Lagoon 3D model:

Explanatory Notes

by D. J. Bombardieri, M. L. Duffett, J. L. Everard and G. V. Cumming

Cover: Views of the Lily-Lagoon 3D Model.

While every care has been taken in the preparation of this report, no warranty is given as to the correctness of the information and no liability is accepted for any statement or opinion or for any error or omission. No reader should act or fail to act on the basis of any material contained herein. Readers should consult professional advisers. As a result the Crown in Right of the State of Tasmania and its employees, contractors and agents expressly disclaim all and any liability (including all liability from or attributable to any negligent or wrongful act or omission) to any persons whatsoever in respect of anything done or omitted to be done by any such person in reliance whether in whole or in part upon any of the material in this report. Crown Copyright reserved.

Abstract

A 3D geological model has been developed for the 20 x 20 km region corresponding to the Lily and Lagoon 1:25,000 map sheets in northwest Tasmania. It expresses a structural and geophysical synthesis developed from recent Mineral Resources Tasmania mapping (Cumming et al., 2022 and Everard et al., 2022). The model is constrained by 3D geophysical modelling using MRT's public domain gravity and magnetic data. Statistically generated sensitivity characterisation is incorporated into 3D model products as a step towards estimating confidence in the spatial variability of geological objects at depth. Inversion results show that calculated gravity and magnetic responses are in reasonable agreement with observations. A product of sensitivity modelling is a new granite surface, which is more detailed when compared to previous iterations. Among the new features to emerge are two granitic cupolas in the vicinity (approximately 1km) of magnetic sources east of the Balfour Shear Zone (BSZ). This result suggests the potential for high-grade vein type lead-zinc-rare earth deposits as proposed by Taheri et al. (2011). An additional product is a 3D representation of magnetic regions represented by a susceptibility shell which could be a tool for exploration. The study also shows that granite is not exposed at the surface east of the BSZ as proposed by Webster (2003). Finally, the outcropping granite at Sandy Cape has a sill-like geometry as proposed by Everard (2005).

Mineral Resources Tasmania

Department of State Growth
www.mrt.tas.gov.au

Lily-Lagoon 3D model

by D. J. Bombardieri, M. L. Duffett, J. L. Everard and G. V. Cumming
Geological Survey Branch - Mineral Resources Tasmania

CONTENTS

1.0 GEOLOGY OF THE STUDY AREA

We present a new 3D model, constrained by gravity, magnetics and detailed surface mapping, of a 20 x 20 km area in the Norfolk Range region of northwest Tasmania. The area is dominated by the lower formations of the Mesoproterozoic lower Rocky Cape Group (RCG), a ≥10 km thick succession of shallow marine shelf deposits with no known base, which was deposited at ~1250-1450 Ma (Halpin et al., 2014). The lower RCG consists mainly of quartzarenite, micaceous sandstone, siltstone and pelite (Seymour et al. in Corbett et al. 2014, p. 42-46).

Most of the sequence is moderately deformed and weakly metamorphosed, but the Balfour Shear Zone (BSZ), a ~35 km long NNW-trending zone of sheared pelite and phyllite, bisects the study area and extends northward. West of the BSZ, the RCG mostly dips east with numerous fault repetitions; to the east is dominated by NE/SW trending open folds (Everard, 2005). Most of the deformation probably occurred during the Cambrian, although Devonian and possibly local Mesoproterozoic deformation is possible. The major formations in the lower RCG are, from the base, the Pedder River Siltstone, Lagoon River Quartzite, Balfour Subgroup and Cowrie Siltstone (Bell, 1972). However, the stratigraphy is not simple, with numerous lateral facies changes. The Lagoon River Quartzite thins and grades into micaceous sandstone eastward and may have a partly transitional relationship with the Balfour Subgroup, which contains lenses of micaceous sandstone and may in turn be a partial facies equivalent of the Cowrie Siltstone (Everard, 2005). The RCG was intruded, mainly east of the BSZ, by the Tayatea Dyke Swarm, which consists of numerous narrow, mostly NNE-trending meta-dolerite dykes dated at 711.1 ± 2.5 Ma (McGregor, 2016). However, these are narrow (mostly ~10-50m), weakly magnetic and have not been modelled. Parallel to the coast in the southwest of the study area, the large (~22 x 4 km) elongate NNW-trending Interview Granite outcrops. The granite intruded the RCG in the Devonian. The small Sandy Cape Granite, just west of the study area, appears to be a more fractionated cupola-like extension of the Interview Granite, and has been dated at 362.4 ±1.9 Ma (Bell, 1972).

The copper deposits in the study area occur along the BSZ and are associated with strong aeromagnetic anomalies. The depth and origin of the anomalies are not known. Quantitative geophysical modelling by Webster (2003) in the southern end of the Balfour copper belt (Line 5a, Webster, 2003; Figures 9 and 10), suggested the source of the high magnetic anomaly in this area is very close to the surface, being less than a few hundreds of metres. Taheri and Bottrill (2005), suggest that the rocks hosting the copper deposits along the belt, which are commonly associated with high magnetic anomalies, lack Devonian granite-related hydrothermal alteration signatures.

2.0 DATA DELIVERY AND VISUALISATION

The model is being distributed as a Geoscience ANALYST project and is described here as such. Geoscience ANALYST is visualisation and communication software for GoCAD® 3D models, made freely available by Mira Geoscience (http://www.mirageoscience.com/).

All spatial objects within the model are referenced to the GDA 94 Datum and the Map Grid of Australia zone 55.

3.0 MODEL CONTENTS

3.1 Cross Sections

The large-scale structure of the area is represented by the six interpretive cross sections. These sections were compiled using field and geophysical data combined with SpheriStat™ profiles and illustrate the structural differences either side of the major northwest to southeast-trending BSZ.

3.2 Deposits

Lily-Lagoon mineral deposit locations were extracted from the MRT mineral occurrence database.

3.3 Granite models

Granite models of the upper contacts of regional granitic intrusions:

- **2003 granite surface:** Interpolated surface generated and modified after Leaman (2003);
- **2023 granite surface:** Interpolated most probable model granite surface developed in this study (see below).

3.4 Input - 3D Geological Modelling

- **Faults:** Surfaces are interpreted from surface mapping and cross sections.
- **Geology Reference Model – Model elements:** The model elements used here are the major formations in the lower RCG, which from the oldest are the Pedder River Siltstone, Lagoon River Quartzite, Balfour Subgroup and Cowrie Siltstone (Bell, 1972), together with the Interview Granite. These units are used in recent 1:25,000 mapping Cumming et al., 2022 and Everard et al., 2022).
- **Observed datasets: Observed TMI response in 2D grid of total magnetic intensity.** Magnetic data were extracted from MRT's publicly available geophysical database. In the Lily-Lagoon area, this

consists largely of the 1996 Arthur-Pieman survey (AGSO/GA P652). It was flown with east–west lines at 200m spacing with a terrain clearance averaging 96m.

The study area hosts numerous magnetic anomalies, mostly within siltstone units with some delineating major fault structures. The most prominent magnetic features are represented by a discontinuous series of north to NNW-trending elongated anomalies (Everard, 2005). Richardson (1994) attributed these anomalies to pyrrhotite and/or magnetite in siltstone. McClenaghan and Seymour (1996) also noted the "noisy character" of the anomalies, observing the NNW-trending fault bounded magnetic anomalous BSZ with other NNE-trending and WNW-trending magnetic structures. Webster (2003) attributed these anomalies to fault related mineralisation sourced from shallow and potentially outcropping S- and I Type granite intrusives. However, Everard (2005) suggested that fieldwork did not support this as the anomalies lack an obvious source and have no consistent grain.

- **Observed gravity response: 2D grid of isostatic residual complete Bouguer gravity anomaly (mGal).** The modelled Bouguer gravity field is a residual recalculated from the isostatic model of Geoscience Australia (Lane et al., 2020). Complete Bouguer anomaly (i.e., terrain-corrected) values are used for modeling. The terrain correction is based on a digital elevation model of 10 m resolution (Duffett, 2018). The study area has reasonable gravity station coverage (typically 1 km) except for the NE quadrant of the Lily 25k map sheet where the coverage is relatively sparse. A strong northwest-trending negative gravity anomaly coincides with the exposed Interview Granite abruptly terminating to the north at 5406000mN. A second strong negative gravity anomaly extends from approximately Mt Norfolk to Mt Hazleton. Leaman (1988) and Webster (2003) suggested that this is related to the elevated terrain of the Norfolk range and attributed the anomaly to an underlying granite spine.

3.5 Output - 3D Geophysical Modelling

- **Calculated datasets**
  - Calculated gravity response: 2D grid of the gravity response (mGal) computed from final model iteration of the inversion.
  - Calculated TMI response: 2D grid of the magnetic response (nT) computed from final model iteration of the inversion;
  - Residual gravity response: 2D grid of the residual gravity response (nT) computed from subtracting the final model iteration from the observed gravity response;
  - Residual TMI response: 2D grid of the residual magnetic response (nT) computed from subtracting the final model iteration from the observed TMI response;
  - Susceptibility shell: A 3D susceptibility shell (ranging between 0.005 to 0.03 SI) extracted from the mean susceptibility probability model.
- **Sensitivity statistics**
  - 3D sectional representation of summary statistics for 50 million inversion iterations. The suite of statistical sensitivity products made available for model interrogation include the following;
  - Entropy, records the volatility of a particular voxel during the inversion. A value of zero indicates low volatility and 1 high volatility;
  - Mean susceptibility, derived from the accumulated accepted inversion proposals/models;
  - Probability of individual unit lithology, the probability of finding an individual geological unit within the whole model space which varies between 0% (black voxels) and 100% (white voxels).

3.6 Vector overlays

- 25k line geology and faults: a vector file of lithological boundaries and faults, extracted from MRT's 1:25,000 seamless geological map coverage;
- Gravity station data: gravity observation points;
- Tenements: vector file of exploration licence areas (EL9/2021, EL25/2020, EL12/2015, EL10/2014) extracted from MRT's register (Jan 3, 2023).

3.7 Digital Elevation Model (DEM)

DEM: Surface topography of the Lily-Lagoon model area. Extracted from MRT's statewide digital elevation model and resampled to 200 metre cells.

3.8 Geology

- **Lily 25K Geology** – image extracted from published MRT 1:25 000 mapping;
- **Lagoon 25K Geology** – image extracted from published MRT 1:25 000 mapping.

4.0 GEOPHYSICAL MODELLING METHODOLOGY - SUMMARY

The geophysical inversion workflow employed represents an evolution of earlier MRT modelling efforts (Bombardieri et al., 2020; Bombardieri et al., 2021).

The Lily-Lagoon 3D model was constructed in 3D GeoModeller™ and built entirely by implicit means, whereby surfaces bounding unit volumes were interpolated from geological observations (stratigraphic and fault contacts, dips, and strikes) via prior geological knowledge encoded in a matrix of rules defining the relative timing of all model components. A useful model can thus be constructed with far fewer user-entered points than explicit modeling. This makes it much easier to modify the model in response to indications from subsequent geophysical modeling.

Model elements include, Proterozoic Rocky Cape Group units, underlying undifferentiated basement and a Devonian granite intrusive corresponding to the interview granite. The level of geological detail incorporated into the model is dictated by likely bulk physical property contrast as well as tectonic, stratigraphic, and practical modelling considerations.

The workflow incorporates geological information in the form of cross-sections representing structural interpretations and petrophysical data in the form of unit rock property density and susceptibility measurements. A "reference model" comprising surfaces representing the various lithologies and fault architecture is first constructed. This model is then discretised in preparation for forward modelling. The 3D model derived to this point is a 'best estimate' synthesis that is consistent with observed gravity and magnetic data. However, as is well recognised for potential field data, this solution is not unique.

Addressing this ambiguity, GeoModeller™ was employed to both refine the inversion and explore the range of similarly plausible possible models, with the goal of estimating the spatial variability of confidence in the model elements. The stochastic exploration algorithm takes a Monte Carlo approach, generating a sequence of linked models starting with the reference model making small "random" changes to the lithological boundaries and physical properties. Model sensitivity is quantified by measuring the evolution of geological bodies via changes to their volume. The commonality and shape ratio probability functions are the two methods used to perform geological tests on proposed cell perturbation or volume change. The commonality constraint aims to preserve a cells original lithology by limiting the degree to which it can vary. This constraint is controlled by a Weibull distribution with a scale parameter ranging from 0.5 (loose) to 0.05 (tight). In contrast, the shape ratio aims to preserve the shape of the original lithology. It is defined as the shape of the lithological unit in the proposed model divided by the shape of the lithological unit in the reference model. The constraint is controlled by a log normal distribution with the scale parameter (i.e., standard deviation) ranging from 0.5 (loose) to 0.05 (tight) (McInerney et al., 2013).

For the Lily-Lagoon gravity inversion, moderate to loose commonality and shape ratio scale parameters were used for geological boundary tests (Appendix 1). A loose constraint (0.5) was used for the Devonian Granite to account for the density contrast between this intrusive and the RCG units. Loose constraints have an impact on the rate of convergence for the joint inversion process by increasing the number of geological acceptances (Bombardieri et al., 2020).

For each iteration, if the geological boundary change is accepted then the geophysical response of the adjusted model (constrained by petrophysical information enforced by statistical distribution laws) is calculated. This model response is assessed, and the proposal is accepted or rejected depending on whether the misfit is improved or maintained below an acceptable threshold (McInerney et al., 2013)

Another parameter used in the inversion is the probability of property change parameter which is set as a ratio. In default mode the ratio is 50/50 meaning there's an equal split between changes made to lithological boundaries and changes to petrophysical properties of the unit. For the Lily-Lagoon gravity inversion a ratio of 1/99 was used with the goal of controlling acceptable levels of geological-boundary variation (Bombardieri et al., 2020).

In contrast, for the magnetic inversion, a ratio of 100/0 was used with the goal of exploring intra-unit susceptibility heterogeneity to account for magnetic anomalies associated with the Rocky Cape Group units. Magnetic data were not used in modifying model geometry due to no one unit having a consistent range of non-zero magnetic properties.

Upon completion of the inversion run, GeoModeller™ carries out an analysis of the ensemble of models that reproduced the observations to an acceptable degree (Bombardieri et al., 2020). Statistical measures were derived from the accumulated accepted inversion proposals/models.

Statistical measures used for this study include the most probable model, entropy, and mean susceptibility.

5.0 RESULTS

For the gravity inversion, approximately 10 million acceptable models were generated for sensitivity analysis. Of these, approximately 9 million consisted of geological unit boundary changes and approximately 1 million consisted of physical rock property changes. The inversion converged after approximately 5 million iterations, with the rms misfit stabilising at approximately 0.7 mGal, close to the noise estimate of the observed data given the model resolution. Results show multiple short to medium scale wavelength negative and positive features in the residual gravity misfit and indicate departures from the bulk mean unit properties. These residuals may arise from alteration, or other processes associated with mineral systems and thus present targets for follow-up exploration. However, such residuals may also be geometric in origin with the inversion not accounting for inaccurate model geometry. A prominent outlier positive residual located (331625 mE and 5408125 mN) within the BSZ and another outlier negative residual located at (331125 mE and 5403125 mN) and may correspond to relatively steep local gradients in the original gravity data, and thus are tentatively attributed to inadequate terrain correction errors, in particular gravity station data (acquired in the pre-GNSS era) or aliasing.

The magnetic inversion converged at approximately 25 million iterations, with the misfit stabilising at approximately 15 nT. The residual misfit was negligible, which is to be expected given the nature of the heterogeneous inversion (i.e., the number of available free parameters used in the inversion). However, positive residuals are present north and east of the exposed Interview Granite. This result suggests additional volumes of anomalously magnetic material (possibly pyrrhotite or magnetite) above and beyond the more magnetic sub-population allowed by the a priori defined bimodal magnetic susceptibility distribution for RCG units (Appendix 1). Edge effects at the northern boundary of the model may reflect regional de-trending and padding algorithms not entirely accounting for sources located just outside the model area

A 3D susceptibility shell (ranging between 0.005 to 0.03 SI) was extracted from the mean susceptibility probability model. The susceptibility shell provides spatial information on potential magnetic sources in the study area.

6.0 SUMMARY

Calculated gravity and magnetic responses of the reference model are in general agreement with observations. A more detailed granite surface compared with previous versions has been produced. Among the new features are two granitic cupolas in the vicinity (approximately 1 km in depth) from magnetic sources east of the BSZ. This suggests that granite-derived fluids are a potential source of metals. Although there is little evidence for a granitic influence on the copper lodes in the area, Taheri et al. (2011) suggest the potential for high-grade vein type lead-zinc-rare earth deposits.

An additional product is a 3D representation of prospective anomalous magnetic regions represented as a susceptibility shell. Anomalies associated with the BSZ and those to the east are generally shallow with a maximum depth of approximately 300 metres, in agreement with Webster (2003). A substantial magnetic zone occurs east of the exposed Interview Granite located southwest of the study area, with a depth ranging from approximately 300 metres at its shallowest, to 3 km below the surface. Our model shows that east of the BSZ, depth to granite is nowhere less than 1 km. This is preferred to the interpretation of Webster (2003), who proposed outcropping granite in this area, contrary to where subsequent field observations have failed to identify either granite or strong contact metamorphic effects. Finally, the proposal that exposed granite at Sandy Cape is sill-like and may represent a cupola rising upward from a northward subsurface continuation, or spine, of the Interview Granite (Everard 2005), is supported by our modelling.

7.0 REFERENCES

Bell, D. H. 1972. *1971–72 Annual Report, EL48/70 and EL49/70, north-western Tasmania joint venture exploration*. Australian Consolidated Industries Ltd, Consolidated Goldfields Australia Ltd, Mt Lyell Mining and Railway Company Ltd, Renison Ltd [TCR72-876].

Bombardieri, D., Duffett, M., McNeill, A., Vicary, M., Paterson, R. 2020. 3D geophysical modeling of the Alberton-Mathinna section of the "Main Slide", Northeast Tasmania. *Interpretation*, 8, T525–T540.

Bombardieri, D., Duffett, M., McNeill, A., Cracknell, M., Reading, A. 2021. Insights and Lessons from 3D Geological and Geophysical Modeling of Mineralized Terranes in Tasmania. *Minerals*, 11(11):1195. https://doi.org/10.3390/min11111195

Cumming, G. V., Everard, J. L. and Jackman, C. J. (compilers). 2022. Digital Geological Atlas 1:25 000 Scale Series. Sheet 3241, *Lily*. Mineral Resources Tasmania.

Duffett, M. 2018. Terrain Correction Tasmania—Results and Implications; *Australian Society of Exploration Geologists Extended Abstracts*, 2018, Sydney, Australia, 1–6.

Everard, J. L. 2005. Reconnaissance geology of the Norfolk Range–Sandy Cape area, northwest Tasmania. *Record Tasmanian Geological Survey*, UR2005_2.

Everard, J. L., Jackman, C. J. and Cumming, G. V. (compilers). 2022. Digital Geological Atlas 1:25 000 Scale Series. Sheet 3240, *Lagoon*. Mineral Resources Tasmania.

Halpin, J. A., Jensen, T., McGoldrick, P., Meffre, S., Berry, R. F., Everard, J. L., Calver, C. R., Thompson, J., Goemann, K., Whittaker, J. M. 2014. Authigenic monazite and detrital zircon dating from the Proterozoic Rocky Cape Group, Tasmania: Links to the Belt-Purcell supergroup, North America. *Precambrian Research*, 250, 50–67.

Leaman, D. E. 1988. EL 27/87 Pieman Head. Regional geophysical review, in: Cromer, W. C. 1989. *EL 27/87 Pieman Head, Tasmania*, Annual Report 10.3.88–10.3.89. New Holland Mining NL [TCR 89-2911].

Leaman, D. E. 2003. Quantitative interpretation of magnetic and gravity data for the Western Tasmanian Regional Minerals Program. Part 1 in: Webster, S. S., Leaman, D. E. 2002. Quantitative interpretation of magnetic and gravity data for the Western Tasmanian Regional Minerals Program. *Record Tasmanian Geological Survey*, UR2002_15.

McInerney, P., Lane, R., Seikel, R., Guillen, A., Gibson, H. and FitzGerald, D. 2013. *Forward modelling and inversion with 3D GeoModeller*. Intrepid Geophysics, Brighton, Victoria. 162 pages. http://www.intrepid-geophysics.com/ig/uploads/manuals/documentation_pdf_geomodeller/pdf_en/GeoModeller_Forward_Modelling_Inversion.pdf (accessed 24 July 2018).

Richardson, R. G. 1994. A geophysical interpretation of the Balfour–Waratah area, northwest Tasmania. *Report Mineral Resources Tasmania,* UR1994_22.

McGregor, C. N. D. 2016. *On the Geochronology of the Tayatea Dyke Swarm of Australia: Identifying Australia's Nearest Laurentian Neighbour in the Proterozoic,* PhD thesis, University of Western Australia.

McClenaghan, M. P. and Seymour, D. B. 1996. Combined interpretation of new aerial-survey geophysical datasets for northwestern Tasmania. *Record Tasmanian Geological Survey,* UR1996_16.

Lane, R. J. L., Wynne, P. E., Poudjom Djomani, Y. H., Stratford, W. R., Barretto, J. A. and Caratori Tontini, F. 2020. 2019 *Australian national gravity grids explanatory notes.* Record 2020/22. Geoscience Australia, Canberra. http://dx.doi.org/10.11636/Record.2020.022

Seymour, D. B., McClenaghan, M. P., Green, G. R., Everard, J. L., Berry, R. F., Callaghan, T., Davidson, G. J., Hills, P. B. 2014. Mid-Palaeozoic orogenesis, magmatism and mineralization. In: Geological Evolution of Tasmania: *Geological Society of Australia Special Publication*, Corbett, K. D., Quilty, P. G., Calver, C. R., Eds., Geological Society of Australia Inc.: Hobart, Australia, 24, 273–362.

Taheri, J. and Bottrill, R. S. 2005. The nature and origins of copper and tin-tungsten deposits in the Balfour - Temma area, northwest Tasmania, *Mineral Resources Tasmania Record,* UR2004_05.

Taheri, J., Bottrill, R. S. and Green, G. R., 2011, A ground-truthing survey in the Interview River area, northwest Tasmania: *Geological Survey Record*, UR2011_01, 1–21.

Webster, S. S. 2003. Quantitative interpretation of magnetic and gravity data for the Western Tasmanian Regional Minerals Program. Part 2 in: Webster, S. S., Leaman, D. E. 2002. Quantitative interpretation of magnetic and gravity data for the Western Tasmanian Regional Minerals Program. *Record Tasmanian Geological Survey*, UR2002_15.

APPENDIX 1

Lily-Lagoon geophysical inversion constraints

Lithology	Input Density (t/m^3)		Commonality	Shape ratio
		1 σ		
Devonian Granite	2.65	0.01	0.5	0.5
Cowrie Siltstone	2.72	0.01	0.05	0.1
Balfour Subgroup	2.72	0.01	0.5	0.5
Lagoon River Quartzite	2.72	0.01	0.2	0.05
Pedder River Siltstone	2.72	0.01	0.3	0.05
Basement	2.72	0.01	0.05	0.05

Lithology	Input Bimodal Distribution: Susceptibility SI						
	Mode 1	1 σ	% Volume		Mode 2	1 σ	% Volume
Devonian Granite	0.0001		100				
Cowrie Siltstone	0.0001	0.02	90		0.02	0.001	10
Balfour Subgroup	0.0002	0.02	85		0.02	0.001	15
Lagoon River Quartzite	0.0002	0.02	95		0.02	0.001	5
Pedder River Siltstone	0.0002	0.02	95		0.02	0.001	5
Basement	0.0002		100				

Tasmanian Government

Mineral Resources Tasmania
PO Box 56 Rosny Park
Tasmania Australia 7018
Ph: +61 3 6165 4800

info@mrt.tas.gov.au www.mrt.tas.gov.au